DOI: 10.48368/bgs-2025.1.n14

Evaluating the impact of radiometric calibration on glacier velocity estimates from Sentinel-1 SAR data: a case study of Livingston island

Adrian Yordanov [1], Vassil Gourev[2], Gergana Georgieva[2]

[1] UACEG, Dept. "Photogrammetry and cartography",, 1 H. Smirnenski Blvd., Sofia 1046, e-mail: a.yordanov_fgs@uacg.bg
[2] Sofia University "St. Kliment Ohridski", Faculty of Physics; James Bouchier Blvd. 5, ggeorgieva@phys.uni-sofia.bg

Abstract
This study evaluates whether applying radiometric calibration to Sentinel-1 GRD (Ground Range Detected) SAR images alters the accuracy of glacier surface velocity estimates obtained with an offset-tracking algorithm. The research focuses on glaciers near the Bulgarian research base on Livingston Island (Antarctica), using available in-situ GNSS (GNSS/-GNSS receiver) velocity measurements as ground truth. Two nearly identical processing chains were implemented in ESA's SNAP software: one including radiometric calibration (producing sigma0), and one without it. All other processing steps and parameters were held constant to isolate the effect of calibration.

Key words: remote sensing, SAR, glacier, velocity maps, radiometric calibration

Introduction
Remote sensing, and SAR in particular, is indispensable for glacier monitoring in polar regions where field data are sparse (Kääb et al., 2016). Offset-tracking on Sentinel-1 GRD products is widely used to estimate surface velocities (Amitrano et al., 2019; Atanasova-Zlatareva et al., 2022; Atanasova M (2023)). Radiometric calibration converts raw pixel values to physically meaningful backscatter (sigma0), potentially influencing the cross-correlation used in offset-tracking. Previous studies have shown mixed sensitivity to calibration; this work quantitatively evaluates the effect on a localized Antarctic setting with GNSS validation.

Study area
Livingston Island is part of the South Shetland Islands archipelago, located west of the Antarctic Peninsula, and is among the actively studied polar regions in West Antarctica. The island covers an area of approximately 798 km², with the majority (87.6%) covered by an ice cap and outlet glaciers. The terrain is predominantly mountainous, with central ridges and plateaus from which numerous glacier streams flow radially towards the northern and southern coasts. In situ measurements of surface ice velocities reveal a wide range, from near-zero values to tens of meters per second, with pronounced seasonality and short-term accelerations.
This study presents results from field observations on the Balkan and Contell glaciers, located in close proximity to the Bulgarian Antarctic Base "St. Kliment Ohridski.
The coordinates of the observed points were determined through GNSS measurements conducted with Trimble Alloy GNSS and Trimble R8s receivers. The Trimble Alloy receiver was used as a base station (positioned at site KOH2), while the Trimble R8s served as a rover station. Long-term measurements in the frontal part of Balkan Glacier were carried out between 2 and 26 January 2023 at a fixed point attached to the ice, located about 100 m from the glacier front and 1318 m from the permanent GPS station KOH2. The coordinates were obtained through static one-hour measurements. The study of ice-flow velocities on Contell Glacier was conducted in January 2025 by repeated measurements (once per week) of stakes arranged in two rows in the upper part of the glacier. The coordinates were determined using 15-minute static sessions.

Methods
This study applies the offset-tracking method to Sentinel-1 Ground Range Detected (GRD) images using two distinct processing chains, both implemented within the SNAP software environment. Both processing chains are illustrated in Figure 1. Both processing chains are designed to enhance co-registration accuracy and subsequently generate high-quality glacier velocity maps. The workflow begins with updating the orbit files, which introduces precise ephemerides and thereby improves the accuracy of the co-registration process. Subsequently, thermal noise removal is applied to correct pixel values affected by system-induced artifacts

(Hajduch et al., 2017). In the first chain, this step is followed by digital elevation model (DEM)-assisted co-registration, whereas in the second chain, radiometric calibration is performed prior to co-registration. Since the study area lies outside the coverage of the SRTM DEM, the ACE30 dataset was employed (E.A.P.R.S. Laboratory, n.d.). A spatial subset is then created to restrict the analysis to the area of interest, after which the offset-tracking algorithm is applied. This method requires several parameters, including grid size (set to 30m), oversample coefficient (set to 16), cross-correlation threshold (0.1 and 0.5), and maximum velocity (2.5m/day according to results from previous studies of the region (Atanasova-Zlatareva and Nikolov, 2022).

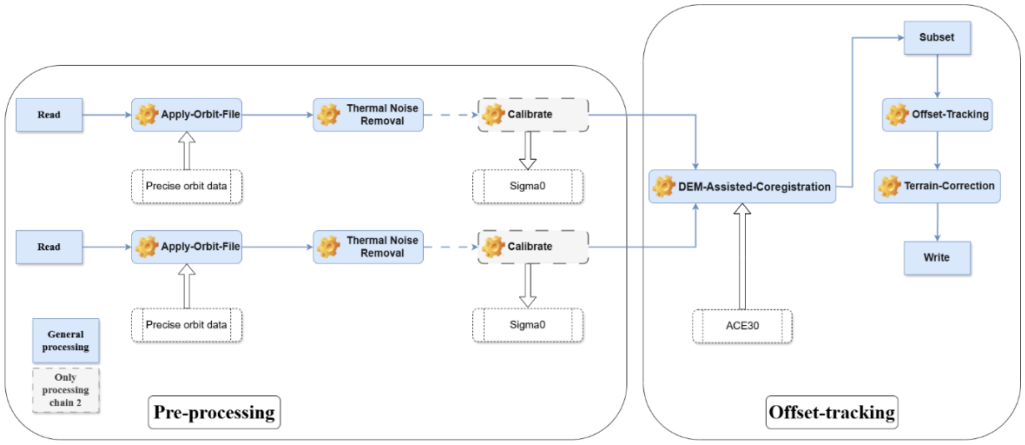


Figure 1 Processing chain for SAR images

The final step of both chains is terrain correction, which projects the output data into the Universal Transverse Mercator (UTM) coordinate system. This correction accounts for distortions introduced by the imaging geometry, ensuring consistency with in-situ measurements, which were also collected in UTM coordinates.
The second processing chain further incorporates radiometric calibration. This procedure corrects the backscattered signal values registered by the sensor and produces one of three possible calibrated products: sigma0, beta0, or gamma0. In this study, sigma0 was selected as it provides terrain-normalized backscatter values. The calibrated sigma0 values were calculated according to equation (1)

$$\sigma^0 = \frac{DN^2}{A_{dn}^2 \cdot K} \cdot \frac{1}{G_{eap}^2} \cdot \left(\frac{R}{R_{ref}}\right)^3 \cdot sin(\alpha) \quad (1)$$

(1)

Where:
$\frac{1}{G_{eap}^2}$ is antenna height correction (EAP)
$\left(\frac{R}{R_{ref}}\right)$ is range signal lost (RSL)
A_{dn} is the final product scale
α is the local incident angle

Results
Overall, calibrated images more often matched GNSS velocities more closely than non-calibrated images, though the magnitude of improvement was typically small.

2023 (representative findings):

- 12-day baseline, low correlation (0.1): differences between GNSS and image velocities were ~0.373 m/day; non-calibrated images were marginally (~0.8 mm/day) closer in this specific test.
- 12-day baseline, high correlation (0.5): differences decreased to ~0.352–0.353 m/day; calibrated images were ~0.44 mm/day closer to GNSS.
- 24-day baseline: typical differences ~0.18 m/day; calibrated images outperformed non-calibrated in low-correlation areas by ~1.69 cm/day; in high-correlation zones the methods converged.

2025 (representative findings):

- First 12-day interval: pointwise differences ranged 0.01–0.275 m/day. Calibrated imagery showed smaller errors at 6 of 9 GNSS points; advantages were typically millimeter-to-centimeter per day.

- Second 12-day and 24-day tests: calibrated products were closer at the majority of GNSS locations, but several individual points favored non-calibrated results (differences often <2 mm/day).

In summary, radiometric calibration nudges velocity estimates toward GNSS by small amounts (mm–cm/day). Effects are strongest in low cross-correlation areas and can vary by and site.

Conclusion

Across both study years and all experimental setups, the application of radiometric calibration generally improved the quality of glacier velocity estimates, although the magnitude of improvement was modest and not consistent across all cases. Given that the computational cost of calibration is minimal compared to the offset-tracking algorithm itself, including it in the processing chain can be advantageous, leading to more reliable results in most situations.

Nonetheless, the absence of calibration—whether due to unavailable calibration constants or limitations of the processing software—does not significantly degrade the accuracy of velocity estimates, as the results remain comparable.

Table 1 Velocity differences between in-situ points and SAR image for 12day and 24day image pairs

Product type	Cross-correlation coefficient	Time period								
		12 days 5.01-17.01			12 days 17.01-29.01			24 days 05.01-29.01		
		GNSS [m/d]	Satellite [m/d]	Difference [m/d]	GNSS [m/d]	Satellite [m/d]	Difference [m/d]	GNSS [m/d]	Satellite [m/d]	Difference [m/d]
Calibrated	0.1	0.06292	0.43633	0.37341	0.04868	0.22836	0.17968	0.06213	0.19764	0.13551
	0.5	0.06292	0.41584	0.35292	0.04868	0.22666	0.17798	0.06213	0.19790	0.13577
Non-Calibrated	0.1	0.06292	0.43554	0.37261	0.04868	0.22667	0.17799	0.06213	0.19792	0.13579
	0.5	0.06292	0.41628	0.35336	0.04868	0.22665	0.17798	0.06213	0.19786	0.13573

Table 2 Image velocity for first 12-day time period of 2025 - cross-correlation 0.1

Name	Date	V(XYH) [m/d]	Vnocal. [m/d]	Vcal. [m/d]	ΔVnocal.(XYH) [m/d]	ΔVcal(XYH) [m/d]
C01-1	20.1.2025	0.01382	0.22416	0.22185	0.21034	0.20804
C02-1	20.1.2025	0.01609	0.20652	0.20611	0.19042	0.19002
C03-1	20.1.2025	0.04530	0.18053	0.18260	0.13523	0.13730
C04-1	19.1.2025	0.08269	0.16447	0.16351	0.08178	0.08083
C12-1	19.1.2025	0.02202	0.27996	0.26501	0.25793	0.24298
C13-1	19.1.2025	0.02190	0.18425	0.19139	0.16235	0.16950
C14-1	19.1.2025	0.03959	0.18186	0.18573	0.14227	0.14614
C15-1	19.1.2025	0.05830	0.10252	0.10046	0.04423	0.04217
C16-1	19.1.2025	0.05906	0.04245	0.04096	-0.01661	-0.01810

Table 3 Image velocity for second 12-day and for 24-day time period of 2025 - cross-correlation 0.1

	Name	Date	V(XYH) [m/d]	Vnocal. [m/d]	Vcal. [m/d]	ΔVnocal.(XYH) [m/d]	ΔVcal(XYH) [m/d]
12-day period	c01	4.2.2025	0.01382	0.17517	0.17437	0.16135	0.16055
	c02	4.2.2025	0.01609	0.23038	0.22929	0.21429	0.21320
	c12	1.2.2025	0.04530	0.20300	0.20192	0.15771	0.15663
	c13	4.2.2025	0.08269	0.31854	0.31593	0.23585	0.23324
	c14	4.2.2025	0.02202	0.36958	0.37154	0.34755	0.34952
24-day period	c01	4.2.2025	0.01716	0.11744	0.11628	0.10027	0.09912
	c02	4.2.2025	0.01548	0.10769	0.10775	0.09221	0.09227
	c12	1.2.2025	0.00973	0.12868	0.12779	0.11895	0.11807
	c13	4.2.2025	0.01501	0.09718	0.09652	0.08217	0.08151
	c14	4.2.2025	0.03980	0.11348	0.11502	0.07368	0.07522

Funding
This study was funded by the Bulgarian Ministry of Education and Science through the National Centre for Polar Studies, and Sofia University "St. Kliment Ohridski" in the framework of the National Program for Polar Studies 2022–2025 (grant numbers 70-25-12/15.01.2024).

References

Amitrano D, Guida R, Di Martino G, Iodice A (2019) Glacier monitoring using frequency domain offset tracking applied to Sentinel-1 images: a product performance comparison. Remote Sensing 11(11):1322 https://doi.org/10.3390/rs11111322

Atanasova M (2023) Ice velocity monitoring of Livingston Island glaciers by time series SAR data. XI National Geophysical Conference, 9 June 2023. https://doi.org/10.48368/bgs-2023.1.N14

Atanasova-Zlatareva M, Nikolov H (2022) Creation of glaciers velocity maps in Livingston Island using Sentinel-1 data. Proceedings Vol. 2, 8th International Conference on Cartography and GIS, 20-25 June 2022, Nessebar, Bulgaria. ISSN 1314-0604. Eds: Bandrova T, Konecny M, Marinova S Earth and Planetary Remote Sensing Laboratory ACE GDEM https://www.cse.dmu.ac.uk/geomatics/products_ace_overview.html [accessed on 19.08.2025]

Hajduch G, Miranda N, Piantanida R, Meadows P, Vincent P, Franceschi N (2017) Thermal denoising of products generated by the S-1 IPF

Miranda N, Meadows PJ (2015) Radiometric calibration of S-1 Level-1 products generated by the S-1 IPF

Kääb A, Winsvold SH, Altena B, Nuth C, Nagler T, Wuite J (2016) Glacier remote sensing using Sentinel-2. Part I: radiometric and geometric performance, and application to ice velocity. Remote Sensing 8(7):598